

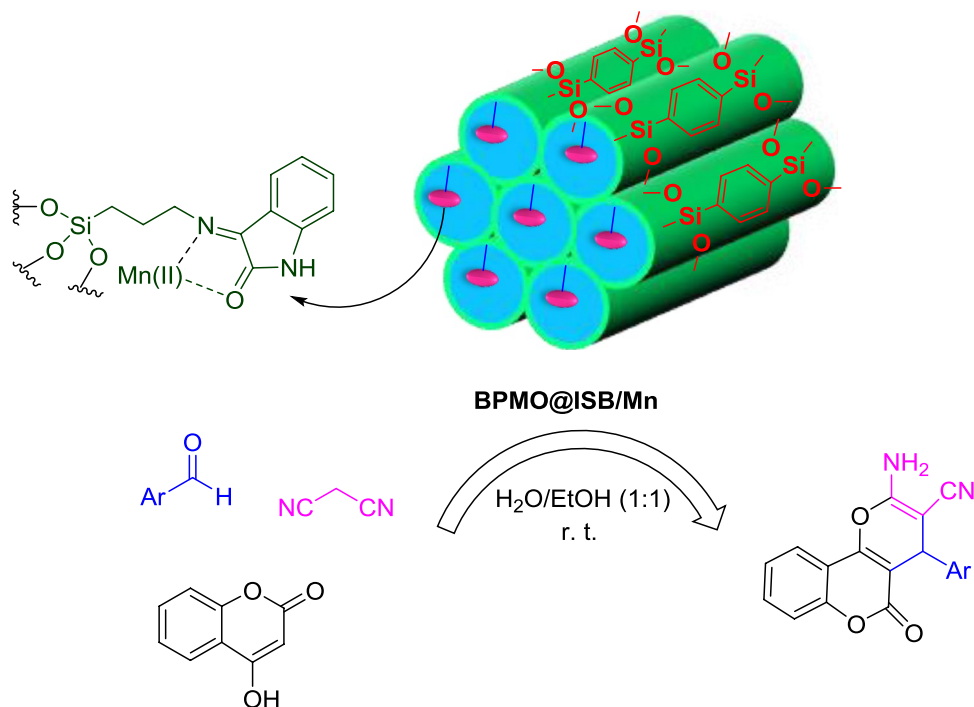
# Phenylene and Isatin Based Bifunctional Mesoporous Organosilica Supported Schiff-Base/Manganese Complex: An Efficient and Recoverable Nanocatalyst

Meysam Norouzi<sup>1</sup> · Dawood Elhamifar<sup>1</sup>

Received: 9 June 2018 / Accepted: 4 January 2019  
© Springer Science+Business Media, LLC, part of Springer Nature 2019

## Abstract

A novel bifunctional periodic mesoporous organosilica supported isatin-Schiff-base/manganese complex [BPMO@ISB/Mn(II)] is prepared, characterized and its catalytic performance is investigated in the synthesis of dihydropyrano[3,2-*c*]chromene derivatives. The BPMO@ISB was prepared via grafting of 3-aminopropyltrimethoxysilane (APTS) on a phenylene based PMO followed by treatment with isatin. The BPMO@ISB was then reacted with  $\text{Mn}(\text{NO}_3)_2 \cdot 4\text{H}_2\text{O}$  to afford the BPMO@ISB/Mn(II) nanocatalyst. This catalyst was characterized using Fourier transform infrared (FT-IR) spectroscopy, thermal gravimetric analysis (TGA), energy-dispersive X-ray (EDX) spectroscopy, scanning electron microscopy (SEM), low angle powder X-ray diffraction (LAPXRD) analysis and transmission electron microscopy (TEM). The BPMO@ISB/Mn(II) nanocatalyst was successfully used in one-pot synthesis of 3,4-dihydropyrano[*c*]chromene derivatives at room temperature. In addition, the stability, recyclability and reusability of designed nanocatalyst were studied under applied conditions.



**Keywords** Bifunctional PMO · Supported isatin · Schiff-base · Manganese nanocatalyst · Dihydropyrano[3,2-*c*]chromenes

Extended author information available on the last page of the article

## 1 Introduction

Due to problems associated with chemical wastes and environmental pollution, the goal of science has recently shifted to design of green chemical processes to reduce and/or remove polluting agents and therefore save environment. One of significant and attracted idea in this matter is replacing of homogeneous catalytic systems with their heterogeneous counterparts [1, 2]. To date a lot of chemical and physical strategies have been developed for immobilization of homogeneous catalysts onto solid supports such as carbon, metal oxides, mesoporous materials, organic–inorganic hybrid materials and polymers [3–7]. Especially, periodic mesoporous organosilicas (PMOs) have emerged as excellent support because of their excellent properties such as high surface area, high capacity for catalyst immobilization, high lipophilicity, high thermal and mechanical stability and uniform distribution of organic and inorganic moieties in their framework [2, 8–13]. These characteristics made PMOs as powerful candidate for a lot of applications in areas of adsorption, catalysis, separation, chromatography and electronics [9–11, 14–18]. More recently, a family of PMOs called bifunctional periodic mesoporous organosilicas (BPMOs) involving functional moieties both in wall and mesopores have created and received exciting attention in green chemistry processes [19–21]. BPMO materials have a lot of applications in heterogonous catalysis, biosensors, enantiomeric separation, light harvesting, drug release and so on [22–32]. To date several BPMOs have been prepared by immobilization of metal and Schiff-base complexes on PMOs for different chemical applications [33–37]. Some of recently developed BPMOs including catalytic centers are Pd-LHMS-3 [25, 38], Ti-LHMS-3 [39], V-LHMS-1 [40], Au/PME-ED [41], Au-HS/SO<sub>3</sub>H-PMO(Et) [42] and Pd-PPh<sub>2</sub>-PMO(Ph) [43] that have been used as catalyst in different organic reactions [8, 19, 21, 44–47]. However, to now there is any report on the preparation of BPMO with isatin moieties in the literature [48–55]. Accordingly, in the present study a novel BPMO nanomaterial containing isatin-Schiff base functional groups has been prepared and applied as efficient support for immobilization of manganese catalyst.

On the other hand, dihydropyrano[3,2-*c*]chromenes are among important and attractive pharmaceutical compounds that exhibit a wide range of biological activities such as myorelaxant, diuretic, analgesic, anticoagulant, anti-tumor, anticancer, cytotoxicity and anti-HIV [56–60]. In addition, these can be used as antimicrobial, anti-tuberculosis agents and cognitive enhancers for the treatment of Alzheimer's disease, neurodegenerative diseases, amyotrophic lateral sclerosis, Parkinson's disease,

Huntington's disease, Down's syndrome, schizophrenia and myoclonus [61–63]. Although several methods have been reported for the synthesis of dihydropyrano[3,2-*c*]chromenes using different catalytic systems, however, some of these protocols suffer from disadvantages of expensive homogenous catalyst, long reaction time, toxic solvent, product separation and catalyst recovery. Therefore, many efforts are being made to develop green and efficient catalytic system for the synthesis of dihydropyrano[3,2-*c*]chromene.

According to aforementioned notes and in continuous of our recent studies in the design, preparation and applications of new supported catalytic systems [52, 64–69], herein a novel bifunctional periodic mesoporous organosilica supported isatin-Schiff-base/manganese (BPMO@ISB/Mn(II)) catalyst is prepared and characterized using several techniques. The BPMO@ISB/Mn(II) nanocatalyst was successfully applied in the one-pot synthesis of dihydropyrano[3,2-*c*]chromene derivatives in aqueous media at room temperature.

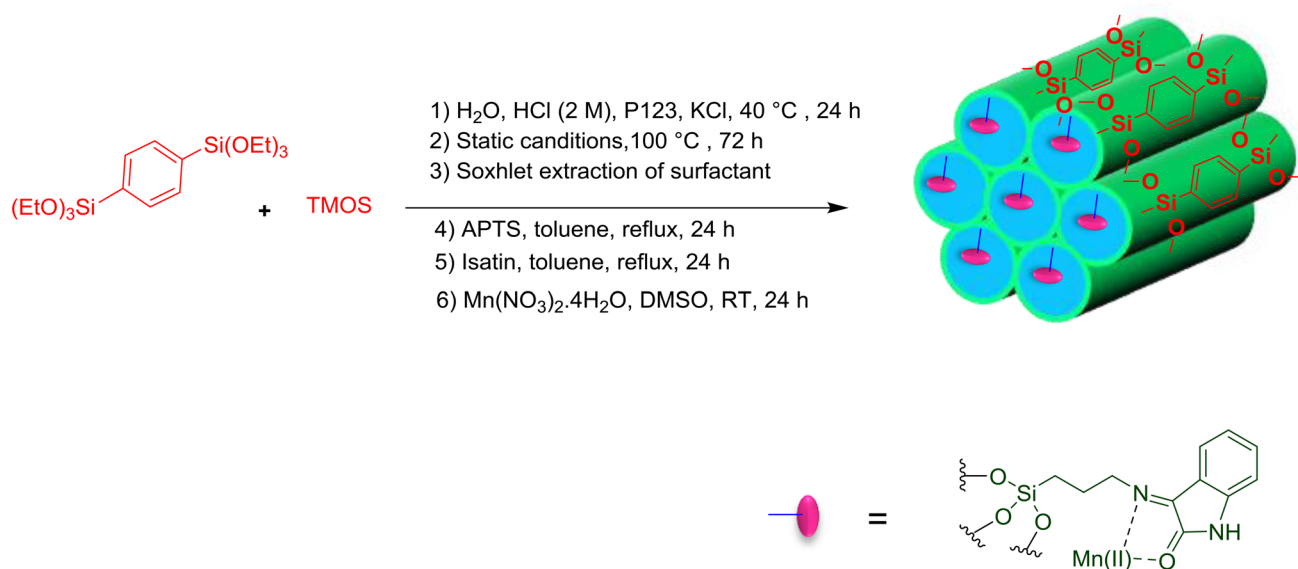
## 2 Experimental Section

### 2.1 General

All chemicals and reagents such as tetramethoxysilane (TMOS), bis(triethoxysilyl)benzene (BTEB), 3-aminopropyltrimethoxysilane (APTS), isatin, pluronic P123, KCl, HCl, malononitrile, 4-hydroxycoumarin and all applied aldehydes were purchased from Merck and Fluka companies. The reaction progress was monitored using TLC. The morphology of the material was investigated using SEM, Philips, XL30 emission electron microscope. TGA was carried out on NETZSCH STA 409 PC/PG apparatus. Low angle powder X-ray diffraction pattern was recorded by a Panalytical model X' Pert Pro focus diffractometer with Cu K $\alpha$  radiation operated at 40 kV and 40 mA. TEM analysis of the catalyst was obtained using FEI TECNAI 12 BioTWIN transmission electron microscope. IR spectra were recorded on a Bruker-Vector 22 spectrometer. Melting points were determined using a KSB1N, Kruss apparatus in open capillary tubes.

### 2.2 Preparation of BPMO@ISB

Firstly, phenylene based periodic mesoporous organosilica (Ph-PMO) was prepared via hydrolysis and co-condensation of bis(triethoxysilyl)benzene (BTEB) and tetramethoxysilane (TMOS) in the presence of pluronic P123 surfactant under acidic conditions (Scheme 1) [51, 65, 70]. It is important to note that the molar ration between these precursors was (TMOS/BTEB, 70:30). Then, Ph-PMO supported



**Scheme 1** Preparation of the BPMO@ISB/Mn(II) nanocatalyst

propylamine (Ph-PMO-Pr-NH<sub>2</sub>) was prepared through chemical grafting of 3-aminopropyl-trimethoxysilane (APTS) onto Ph-PMO [51]. Typically, 1 g of Ph-PMO was added in dry toluene (30 mL) and stirred at room temperature. After complete dispersion of Ph-PMO, APTS (4 mmol) was added into reaction vessel and resulted mixture was refluxed for 24 h under argon atmosphere. After cooling to room temperature, the obtained solid was collected through filtration, washed several times with ethanol and then dried at 65 °C for 10 h to yield Ph-PMO-Pr-NH<sub>2</sub>. After that, the Ph-PMO supported isatin-Schiff-base (BPMO@ISB) was prepared [35, 37] as following: Ph-PMO-Pr-NH<sub>2</sub> (1 g) was well dispersed in toluene (20 mL) and isatin (8 mmol) was added. The resulting mixture was refluxed for 24 h under argon atmosphere. Finally, the obtained mixture was cooled to room temperature, filtered, washed completely with ethanol and dried at 70 °C for 12 h to give a solid material called BPMO@ISB.

### 2.3 Preparation of BPMO@ISB/Mn(II) nanocatalyst

For the preparation of BPMO@ISB/Mn(II), the BPMO@ISB (1 g) was added in DMSO (20 mL) and stirred at room temperature. After complete dispersion of this nanomaterial, a prepared DMSO solution of Mn(NO<sub>3</sub>)<sub>2</sub>·4H<sub>2</sub>O (4 mmol) was added in the reaction vessel and it was stirred for 24 h at room temperature under argon atmosphere. The resulted mixture was then filtered and washed with absolute ethanol to remove unreacted manganese nitrate. The obtained solid was dried at 70 °C for 10 h to deliver a uniform powder called BPMO@ISB/Mn(II) nanocatalyst. The loading of the manganese was obtained to be 0.22 mmol Mn/g by the

means of the Mn-content obtained from inductively coupled plasma/optical emission spectroscopy (ICP-OES).

### 2.4 Synthesis of Dihydropyrano[3,2-c]chromene Derivatives in the Presence of BPMO@ISB/Mn(II) Nanocatalyst

A mixture of aldehyde (1 mmol), 4-hydroxycoumarin (1 mmol), malononitrile (1.2 mmol), and BPMO@ISB/Mn(II) (20 mg) were added in aqueous ethanol (H<sub>2</sub>O/EtOH, 1:1, 5 mL). This was magnetically stirred at room temperature for appropriate time indicated in Table 3. After completion of the reaction, monitored by TLC, the resulted mixture was dissolved in warm ethanol (10 mL) and the catalyst was separated by filtration. Then, the pure products were obtained after recrystallization in ethanol.

### 2.5 Procedure for the Recovery of BPMO@ISB/Mn(II)

To study the recoverability of the BPMO@ISB/Mn(II) nanocatalyst, benzaldehyde (1 mmol), 4-hydroxycoumarin (1 mmol), malononitrile (1.2 mmol) and BPMO@ISB/Mn(II) (20 mg) were added in aqueous ethanol (H<sub>2</sub>O/EtOH, 1:1) while stirring at room temperature. After completion of the reaction, the catalyst was separated by simple filtration, washed and dried at 70 °C for 2 h. The recovered catalyst was then reused in the next run charged with the same amounts of starting materials under above mentioned conditions. These steps were repeated and it was found that the catalyst could be recovered and reused at least 5 times without significant decrease in efficiency.

## 2.6 Procedure for the Filtration Test

Filtration test was performed to show whether active manganese catalyst is leached from the solid material during the reaction or not. For this purpose, the experiment was performed in a water/ethanol solution containing benzaldehyde (1 mmol), 4-hydroxycoumarin (1 mmol), malononitrile (1.2 mmol) and BPMO@ISB/Mn(II) (20 mg) at room temperature. After about 50% of the reaction was completed, the BPMO@ISB/Mn(II) nanocatalyst was separated using simple filtration and then the residue was allowed to progress at room temperature for 2 h.

## 3 Results and Discussion

For the preparation of BPMO@ISB/Mn(II) nanocatalyst, firstly phenylene-based periodic mesoporous organosilica (Ph-PMO) was synthesized via surfactant directed simultaneous hydrolysis and co-condensation of bis(triethoxysilyl) benzene and tetramethoxysilane under acidic conditions. This was then modified with 3-aminopropyltrimethoxysilane to afford Ph-PMO-Pr-NH<sub>2</sub>. The bifunctional PMO supported isatin-Schiff-base (BPMO@ISB) was then prepared by treatment of Ph-PMO-Pr-NH<sub>2</sub> with isatin in toluene under reflux conditions. After that, the BPMO@ISB was applied as effective support for successful immobilization of manganese to deliver BPMO@ISB/Mn(II) nanocatalyst (Scheme 1). As shown in Scheme 1, during the first steps the supported amine moieties reacted with carbonyl groups of isatin to form Schiff-base ligands that are appropriate for immobilization of metallic sites. In the next step, the manganese salt (Mn(NO<sub>3</sub>)<sub>2</sub>·4H<sub>2</sub>O) was reacted with supported isatin moieties to prepare isatin-Schiff-base/Mn complex.

The physicochemical properties of the BPMO@ISB/Mn(II) nanocatalyst were studied using FT-IR, SEM, TEM, TGA and EDX techniques. Firstly, the FT-IR analysis of the Ph-PMO, Ph-PMO-P123 and BPMO@ISB/Mn(II) was performed to study the functionality of the materials in the range of 400–4000 cm<sup>-1</sup> (Fig. 1). For all materials, the characteristic bands of aromatic C=C, aliphatic C–H, aromatic C–H and H–O stretching vibrations were appeared, respectively, at 1556, 2944, 3095 and 3400 cm<sup>-1</sup>. Moreover, for these samples the asymmetric and symmetric stretching vibrations of Si–O–Si bonds were observed at 956 and 1070 cm<sup>-1</sup>. For Ph-PMO-P123 the bands observed at 2920 and 2850 were due to the aliphatic C–H stretching vibrations of P123 surfactant (Fig. 1a). Interestingly, for Ph-PMO (Fig. 1b) and BPMO@ISB/Mn(II) (Fig. 1c), the latter peaks were eliminated indicating successful removal of surfactant during extraction process. It is also important to note that for BPMO@ISB/Mn(II) sample the peak

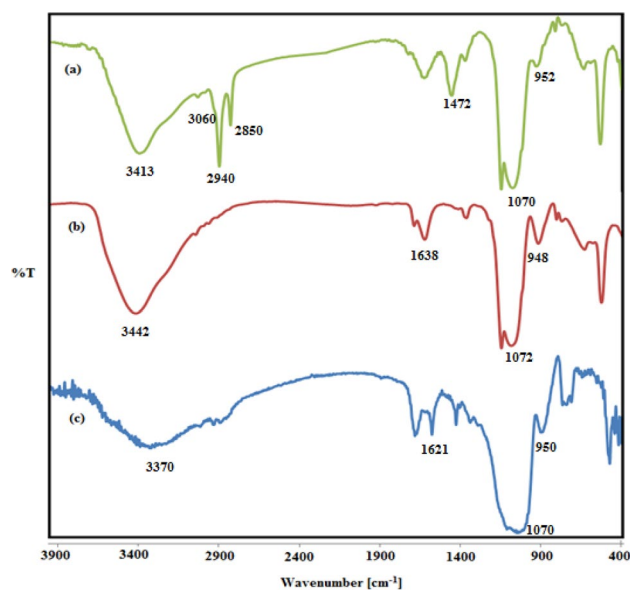


**Fig. 1** FTIR spectra of **a** Ph-PMO-P123, **b** Ph-PMO and **c** BPMO@ISB/Mn(II) nanomaterials

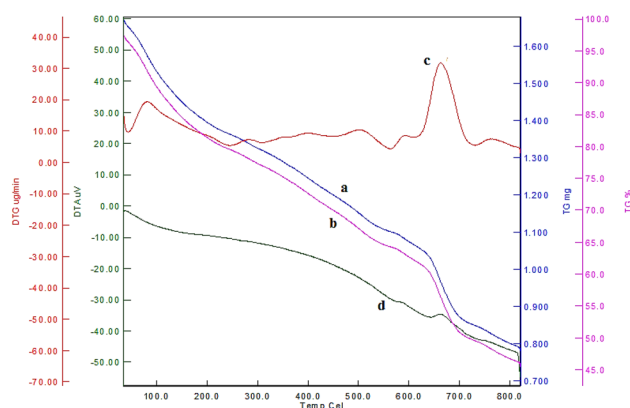


**Fig. 2** Thermal gravimetric analysis (TGA based on mg, **a**), (based on percent, **b**), derivative TG (DTG, **c**) and differential thermal analysis (DTA, **d**) curves of the BPMO@ISB/Mn(II) nanocatalyst

cleared at 1621 is assigned to C=N bond confirming successful formation of Schiff-base (SB) complex onto material surface (Fig. 1c).

Thermal stability of the BPMO@ISB/Mn(II) nanocatalyst was evaluated using thermal gravimetric analysis (TGA). As seen in Fig. 2, the BPMO@ISB/Mn(II) undergoes the first weight loss below 100 °C which is due to removal of adsorbed or trapped water and alcoholic solvents. The main weight loss appearing between 270 and 800 °C is corresponded to the decomposition of organic groups (propylamine and isatin) grafted onto PMO surface and also phenylene moieties incorporated in the body of BPMO@ISB/Mn(II). These results indicate high thermal stability of the designed nanocatalyst.

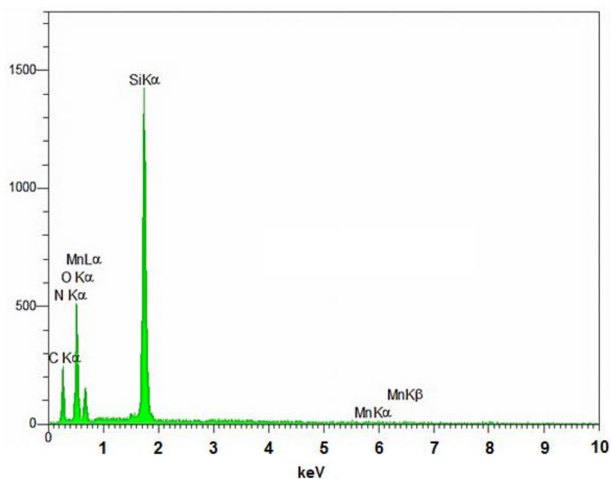


**Fig. 3** EDX spectrum of the BPMO@ISB/Mn(II) nanocatalyst

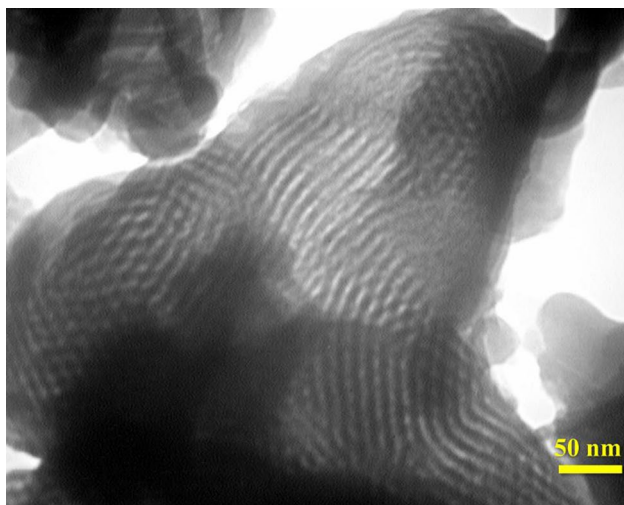


**Fig. 4** TEM image of the BPMO@ISB/Mn(II) nanocatalyst

The EDX spectrum of BPMO@ISB/Mn(II) nanocatalyst (Fig. 3) showed the signals of carbon, nitrogen, oxygen, silicon and manganese. This result is in good agreement with the results of TG and FTIR analyses confirming successful incorporation and/or immobilization of phenylene, propyl-isatin and manganese moieties onto/into material framework.

The TEM image of BPMO@ISB/Mn(II) nanocatalyst demonstrated a structure with well-ordered channels that proves the presence of two dimensional mesostructure with high regularity for the material (Fig. 4). The SEM image also clearly showed the presence of high-ordered spherical particles for the BPMO@ISB/Mn(II) catalyst (Fig. 5). These results successfully confirm high ability and efficiency of the designed catalyst in the catalytic process.

The low angle powder X-ray diffraction (LAPXRD) analysis of both BPMO@SB and BPMO@SB/Mn(II)

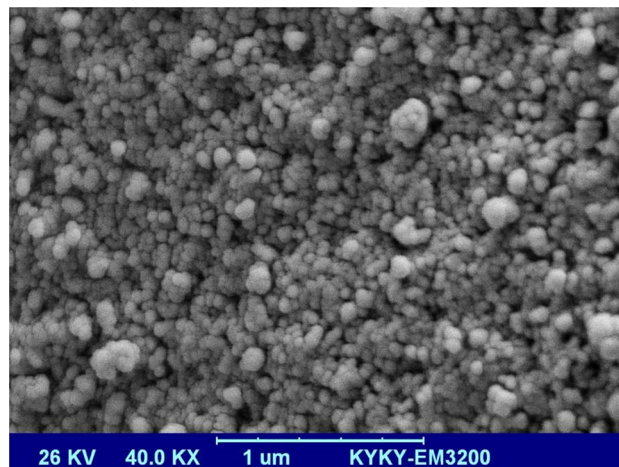


**Fig. 5** SEM image of BPMO@ISB/Mn(II) nanocatalyst

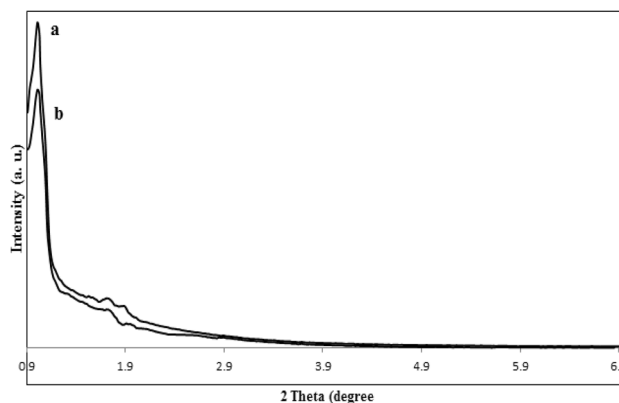


**Fig. 6** Low-angle X-ray diffraction analysis of **a** BPMO@SB and **b** BPMO@SB/Mn(II) nanomaterials

nanocatalyst showed a peak at  $2\theta = 1.1^\circ$  indicating a mesoporous structure for these materials (Fig. 6). The lower intensity of aforementioned peak for the BPMO@SB/Mn(II) catalyst confirms successful immobilization of manganese moieties onto BPMO@SB surface.

The BET experiment of the BPMO@ISB, BPMO@ISB/Mn(II) and recovered BPMO@ISB/Mn(II) [RBPMO@ISB/Mn(II)] materials were also performed and according to this analysis, the BET surface area for BPMO@ISB, BPMO@ISB/Mn(II) and RBPMO@ISB/Mn(II) was  $647 \text{ m}^2/\text{g}$ ,  $553 \text{ m}^2/\text{g}$  and  $462 \text{ m}^2/\text{g}$ , respectively (Table 1). Moreover, total pore volume was calculated to be 1.27, 1.20 and  $1.02 \text{ cm}^3/\text{g}$  for the BPMO@ISB, BPMO@ISB/Mn(II) and RBPMO@ISB/Mn(II) materials (Table 1). The decrease in the surface area and pore diameter of modified BPMO@ISB is corresponded to the immobilization of APTS, isatin and Mn(II) complex onto the mesoporous pores. These results are in good agreement with TEM and PXRD analyses and

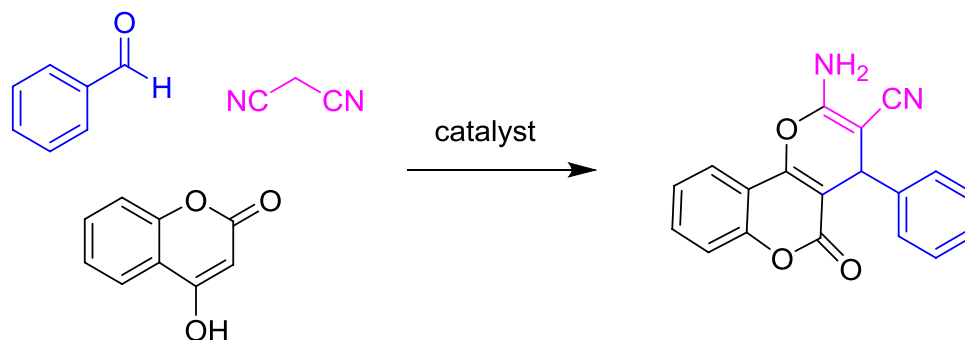
**Table 1** Structural parameters of BPMO@ISB, BPMO@ISB/Mn(II) and RBPMO@ISB/Mn(II) determined from BET experiments

Sample	BET surface area (m <sup>2</sup> g <sup>-1</sup> )	Pore diameter (nm)	Pore volume (cm <sup>3</sup> g <sup>-1</sup> )
BPMO@ISB	647	5.1	1.27
BPMO@ISB/Mn(II)	553	4.5	1.20
RBPMO@ISB/Mn(II)	462	3.9	1.02

successfully confirm the presence of a well-ordered meso-structure for the materials. It is also important to note that the decrease in the surface area, pore volume and pore diameter for the recovered catalyst in comparison with its parent is attributed to partial saturation of mesochannels with starting materials and reaction products.

After characterization, the catalytic activity of the BPMO@ISB/Mn(II) was investigated in the synthesis of dihydropyrano[3,2-*c*]chromene derivatives. For this, the condensation of benzaldehyde with malononitrile and 4-hydroxycoumarin was selected as a model reaction. The

reaction conditions were optimized to determine a suitable catalyst loading and solvent (Table 2). At first, the reaction was performed without catalyst at room temperature (Table 2, entry 1) that no considerable product was obtained. Where 10 mg of catalyst was used, about 53% yield was resulted (Table 2, entry 2). The best conversion was obtained in the presence of 20 mg of catalyst indicating the key role of catalyst loading in the reaction progress (Table 2, entry 3). In the next, the effect of solvent in the reaction progress was studied (Table 2, entries 4–10). Among different solvents, the best result was obtained in aqueous ethanol (H<sub>2</sub>O/EtOH, 1:1, Table 2, entry 9). Also, the effect of volume of solvent showed that the use of 5 mL gives the best conversion (Table 2, entries 8–10). Accordingly the use of 20 mg of catalyst at room temperature in aqueous ethanol were selected as optimum conditions. To study the individual impact of manganese species during this catalytic process, the efficiency of the BPMO@ISB/Mn(II) was compared with those of Ph-PMO-Pr-NH<sub>2</sub> and BPMO@ISB nanomaterials. The results showed that in the presence of both Ph-PMO-Pr-NH<sub>2</sub> and BPMO@ISB materials, the reaction is not performed

**Table 2** The effect of catalyst loading and solvent in the preparation of dihydropyrano[3,2-*c*]chromenes

Entry	Catalyst	Catalyst (mg)	Time (min)	Solvent	Yield (%) <sup>a</sup>
1	–	–	120	–	–
2	BPMO@ISB/Mn(II)	10	15	–	37
3	BPMO@ISB/Mn(II)	15	15	–	54
4	BPMO@ISB/Mn(II)	20	15	–	76
5	BPMO@ISB/Mn(II)	20	15	EtOH (5 mL)	80
6	BPMO@ISB/Mn(II)	20	15	CH <sub>3</sub> CN (5 mL)	50
7	BPMO@ISB/Mn(II)	20	15	H <sub>2</sub> O (5 mL)	88
8	BPMO@ISB/Mn(II)	20	15	H <sub>2</sub> O/EtOH (3 mL)	90
9	BPMO@ISB/Mn(II)	20	15	H <sub>2</sub> O/EtOH (5 mL)	95
10	BPMO@ISB/Mn(II)	20	15	H <sub>2</sub> O/EtOH (7 mL)	95
11	Ph-PMO-Pr-NH <sub>2</sub>	20	15	H <sub>2</sub> O/EtOH (5 mL)	<5
12	BPMO@ISB	20	15	H <sub>2</sub> O/EtOH (5 mL)	<5

<sup>a</sup>Conditions: benzaldehyde (1 mmol), malononitrile (1.2 mmol) and 4-hydroxycoumarin (1 mmol) at room temperature

<sup>a</sup>Isolated yield

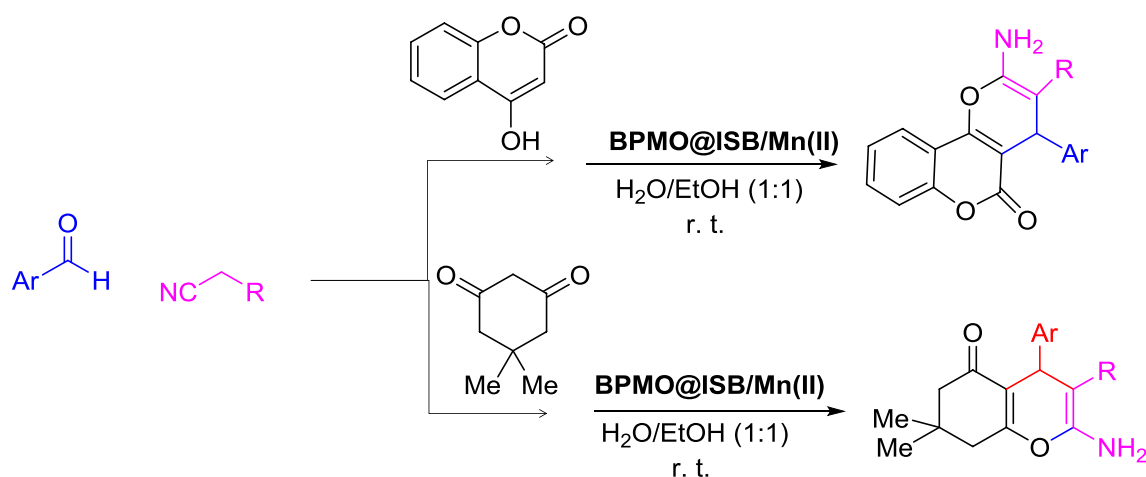
and only a low yield of product is obtained (Table 2, entry 9 vs. entries 11 and 12). This confirms that the reaction is mainly catalyzed by supported manganese species.

In optimized conditions, the scope and generality of this process were further studied with a set of different aldehydes containing either electron-withdrawing (4-nitobenzaldehyde, 4-cyanobenzaldehyde, 2-furfural and 4-fluorobenzaldehyde) and electron-donating (such as 4-methylbenzaldehyde) substituents. As shown, both of these substrates delivered corresponding coupling products in high to excellent yields without formation any side product in very short reaction time (Table 3). It is important to note that this reaction is initiated by manganese complex assisted Knoevenagel condensation to provide cyanocinnamitrile intermediate

[51]. Then, Micheal addition of cyanocinnamitrile with 4-hydroxy coumarin, followed by cyclization and rearrangement provides desired product [71, 72]. In order to extend the scope of the present method and to evaluate the efficiency of the BPMO@ISB/Mn(II) catalyst for organic reactions, the replacement of 4-hydroxy-co-mamarin with dimedone under the same conditions as above provided corresponding tetrahydrobenzo [*b*] pyran derivatives in high yields and short reaction times (Table 3, entries 10 and 11).

Since recovery and reusability of catalyst in industrial and commercial applications as well as in green chemistry are very important, in the next the recoverability and reusability of the BPMO@ISB/Mn(II) nanocatalyst were studied in the synthesis of dihydropyrano [3,2-*c*] chromenes. In this

**Table 3** Preparation of dihydropyrano[3,2-*c*]chromenes and tetrahydrobenzo[*b*]pyran derivatives in the presence of BPMO@ISB/Mn(II) nanocatalyst



Entry	Ar	R	Time (min)	Yield (%) <sup>a</sup>	TON <sup>b</sup>	Mp (°C)	M.P (°C) <sup>Ref</sup>
1	C <sub>6</sub> H <sub>5</sub>	CN	15	95	216	255–257	256–258 [73]
2	4-MeC <sub>6</sub> H <sub>5</sub>	CN	25	88	200	259–261	258–260 [74]
3	4-CNC <sub>6</sub> H <sub>5</sub>	CN	10	93	211	223–226	224–226 [75]
4	4-FC <sub>6</sub> H <sub>5</sub>	CN	10	92	209	260–262	262–263 [73]
5	3-NO <sub>2</sub> C <sub>6</sub> H <sub>5</sub>	CN	10	92	209	259–262	262–264 [76]
6	4-NO <sub>2</sub> C <sub>6</sub> H <sub>5</sub>	CN	8	95	216	255–256	256–258 [73]
7	4-BrC <sub>6</sub> H <sub>5</sub>	CN	15	90	205	254–256	254–256 [74]
8	2-furfural	CN	15	90	204	251–254	253–255 [77]
9	4-NO <sub>2</sub> C <sub>6</sub> H <sub>5</sub>	COOEt	18	92	209	242–244	241–243 [73]
10 <sup>c</sup>	4-CNC <sub>6</sub> H <sub>5</sub>	CN	10	95	216	228–230	226–228 [78]
11 <sup>c</sup>	4-MeC <sub>6</sub> H <sub>5</sub>	CN	15	92	209	217–220	216–218 [79]

Conditions: aldehyde (1 mmol), malononitrile (1.2 mmol), 4-hydroxycoumarin (1 mmol) and BPMO@ISB/Mn(II) catalyst (20 mg, 0.44 mol%) in aqueous ethanol (1:1, H<sub>2</sub>O/EtOH) at room temperature

<sup>a</sup>Isolated yields

<sup>b</sup>TON turnover number (defined as mmol of product/mmol of catalyst)

<sup>c</sup>Aldehyde (1 mmol), malononitrile (1.2 mmol), dimedone (1 mmol) and BPMO@ISB/Mn(II) catalyst (20 mg) in aqueous ethanol (1:1, H<sub>2</sub>O/EtOH) at room temperature

part of our study, it was found that the BPMO@ISB/Mn(II) nanocatalyst could be recycled at least five times without considerable loss in its activity (Fig. 7).

The FT-IR spectrum of the recovered BPMO@ISB/Mn(II) nanocatalyst (Fig. 8a) was also performed to investigate the stability of Schiff-base moieties during reaction process and the result was compared with the fresh BPMO@ISB/Mn(II) nanocatalyst (Fig. 8b). Interestingly, both of these spectra showed the presence of a band at 1621 corresponding to C=N bond of Schiff-base group indicating the stability of this ligand under applied reaction conditions.

In the next, the SEM analysis of the recovered BPMO@ISB/Mn(II) nanocatalyst was performed and the result was compared with the SEM image of the fresh catalyst. As shown, the morphology of the recovered catalyst is approximately the same as fresh catalyst indicating high stability of the material structure during catalytic process (Figs. 5 vs. 9).

To investigate the efficacy of the BPMO@ISB/Mn(II) catalyst in the synthesis of dihydropyrano [3,2-*c*]chromenes, we compared the results obtained in this work with those reported in the literature mediated by other catalysts (Table 4). The results showed that the new catalyst is equally or more efficient catalyst than previously reported systems. The advantages of the present work in comparison to previously reported ones are high surface area, high uniformity and stability of the support, high lipophilicity of the mesochannels simplifying well-diffusion of organic substrates and mild reaction conditions that make this method from the green chemistry point of view more environmentally friendly.

Although no significant decrease in the efficiency of the catalyst was observed after the reusability test, to show whether any BPMO@ISB/Mn(II) complex is leached from the BPMO@ISB surface during the reaction progress, a filtration test was performed in the model reaction after ~50% of the coupling reaction was completed. For this, the BPMO@ISB/Mn(II) nanocatalyst was separated using

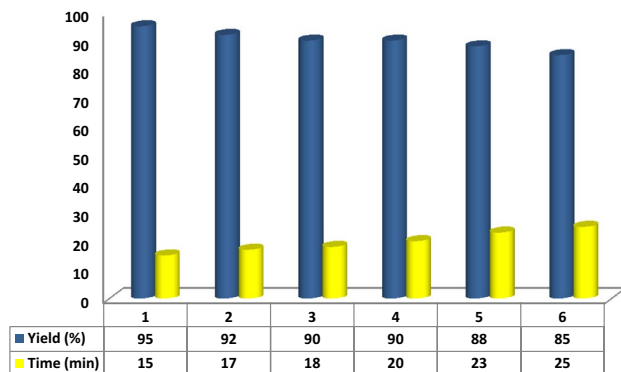


**Fig. 7** Reusability of the BPMO@ISB/Mn(II) nanocatalyst in the synthesis of dihydropyrano [3,2-*c*]chromenes

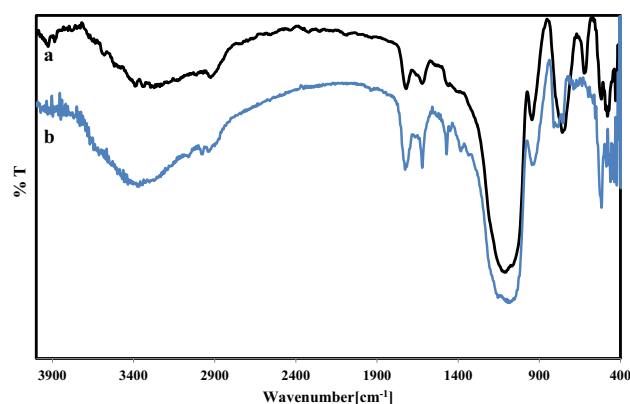


**Fig. 8** FTIR spectrum of **a** recovered BPMO@ISB/Mn(II) and **b** fresh BPMO@ISB/Mn(II) nanocatalyst

simple filtration and then reaction mixture was allowed to continue under applied conditions. Interestingly, after 2 h only a trace conversion of starting materials was found.

The latter studies successfully confirm high recoverability, reusability, reactivity, stability and durability of desired catalyst under applied conditions.

## 4 Conclusion

In summary, for the first time a novel manganese containing phenylene and isatin-Schiff-base based bifunctional PMO [BPMO@ISB/Mn(II)] was prepared and characterized. The FT-IR, TG and EDX analyses successfully confirmed well-incorporation and immobilization of organic and inorganic moieties into/onto material framework. The TEM image demonstrated the presence of high-ordered two-dimensional mesostructure for this catalyst. The SEM image also showed

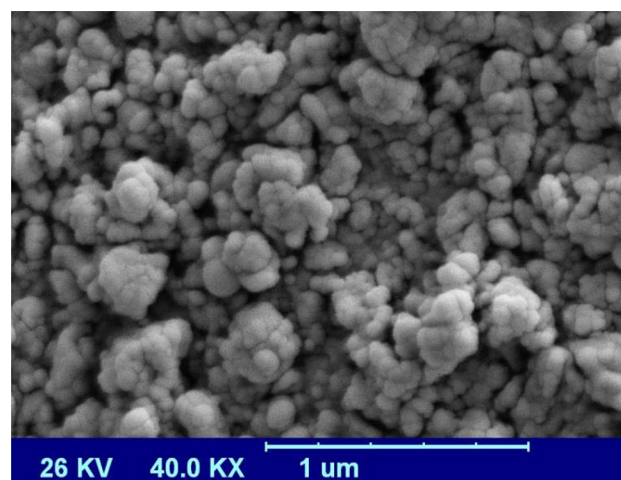


**Fig. 9** SEM image of the recovered BPMO@ISB/Mn(II) nanocatalyst

**Table 4** Comparison of activity of BP MO@ISB/Mn(II) catalyst with the previously reported catalytic systems in the synthesis of dihydropyrano [3,2-*c*]chromenes

Entry	Catalyst	Conditions	References
1	Fe <sub>3</sub> O <sub>4</sub> @SiO <sub>2</sub> -imid-PMA	H <sub>2</sub> O, reflux or ultrasonic	[80]
2	SBPPSP <sup>a</sup>	H <sub>2</sub> O/EtOH, reflux	[81]
3	CTMAB-bentonite <sup>b</sup>	H <sub>2</sub> O/EtOH, 70 °C	[82]
4	RuBr <sub>2</sub> (L) <sub>4</sub> <sup>c</sup>	MeOH, reflux	[83]
5	SiO <sub>2</sub> /H <sub>3</sub> PW <sub>12</sub> O <sub>40</sub>	Solvent free, 80 °C	[84]
6	γ-Fe <sub>2</sub> O <sub>3</sub> @HAp-Si-(CH <sub>2</sub> ) <sub>3</sub> -AMP <sup>d</sup>	H <sub>2</sub> O, reflux	[85]
7	Polypyrrole/Fe <sub>3</sub> O <sub>4</sub> /CNT <sub>e</sub>	Solvent free, 90 °C	[86]
8	BP MO@ISB/Mn(II)	H <sub>2</sub> O/EtOH, r.t	This work

<sup>a</sup>Silica-bonded *N*-propylpiperazine sodium *n*-propionate<sup>b</sup>Surfactant modified bentonite<sup>c</sup>Ru(II) complexes bearing tertiary phosphine ligands<sup>d</sup>Magnetic hydroxyapatite encapsulated γ-Fe<sub>2</sub>O<sub>3</sub> supported (2-aminomethyl) phenol<sup>e</sup>Carbon nanotube (CNT)

the presence of particles with spherical morphology for this material. The BP MO@ISB/Mn(II) was successfully applied as an effective and recoverable catalyst for the synthesis of dihydropyrano [3,2-*c*]chromene derivatives and gave products in high to excellent yields at room temperature and short times. This catalyst was easily recovered and reused several times with keeping its performance in aqueous ethanol as green solvent. The high efficiency of the present catalytic system is attributed to good mesoporosity of the designed catalyst, high stability and durability of active sites, the use of green solvent and performing reaction at very short times at room temperature.

**Acknowledgements** The authors thank the Yasouj University and the Iran National Science Foundation (INSF) for supporting this work.

## References

- Zhang Y, Zhao Y, Xia C (2009) *J Mol Catal A* 306(1–2):107–112
- Wight A, Davis M (2002) *Chem Rev* 102:3589–3614 102
- Nikoorazm M, Ghorbani-Choghamarani A, Noori N, Tahmasbi B (2016) *Appl Organomet Chem* 30:843–851
- Zhang L, Feng C, Gao S, Wang Z, Wang C (2015) *Catal Commun* 61:21–25
- Jin M, Park J-N, Shon JK, Kim JH, Li Z, Park Y-K, Kim JM (2012) *Catal Today* 185:183–190
- Ghosh S, Dey R, Ahammed S, Ranu BC (2014) *Clean Technol Environ Policy* 16:1767–1771
- Veisi H, Kordestani D, Faraji AR (2014) *J Porous Mater* 21:141–148
- Díaz U, Brunel D, Corma A (2013) *Chem Soc Rev* 42:4083–4097
- Inagaki S, Guan S, Fukushima Y, Ohsuna T, Terasaki O (1999) *J. Am. Chem. Soc.* 9611-14 121
- Asefa T, MacLachlan MJ, Coombs N, Ozin GA (1999) *Nature* 402:867–871
- Melde BJ, Holland BT, Blanford CF, Stein A (1999) *Chem Mater* 11:3302–3308
- Stein A (2003) *Adv Mater* 15:763–775
- Wahab MA, Beltramini JN (2015) *RSC Adv* 5:79129–79151
- Hatton B, Landskron K, Whitnall W, Perovic D, Ozin GA (2005) *Acc Chem Res* 38:305–312
- Hunks WJ, Ozin GA (2005) *J Mater Chem* 15:3716–3724
- Yaghoubi A, Dekamin MG (2017) *Chem Sel* 2:9236–9243
- Dekamin MG, Arefi E, Yaghoubi A (2016) *RSC Adv* 6:86982–86988
- Yaghoubi A, Dekamin MG, Karimi B (2017) *Catal Lett* 147:2656–2663
- Xia LY, Zhang MQ, Rong MZ, Xu WM (2010) *Phys Chem Chem Phys* 12:10569–10576
- Olkhovoyk O, Pikus S, Jaroniec M (2005) *J Mater Chem* 15:1517–1519
- Alauzun J, Mehdi A, Reyé C, Corriu RJ (2007) *J Mater Chem* 17:349–356
- Johnson-White B, Zeinali M, Shaffer KM, Patterson CH, Charles PT, Markowitz MA (2007) *Biosens Bioelectron* 22:1154–1162
- Inagaki S, Guan S, Yang Q, Kapoor MP, Shimada T (2008) *Chem Commun.* <https://doi.org/10.1039/b714163g>
- Takeda H, Goto Y, Maegawa Y, Ohsuna T, Tani T, Matsumoto K, Shimada T, Inagaki S (2009) *Chem Commun* 6032–6034
- Modak A, Mondal J, Aswal VK, Bhaumik A (2010) *J Mater Chem* 20:8099–8106
- Fryxell GE, Liu J, Hauser TA, Nie Z, Ferris KF, Mattigod S, Gong M, Hallen RT (1999) *Chem Mater* 11:2148–2154
- Lu Y, Fan H, Doke N, Loy DA, Assink RA, LaVan DA, Brinker CJ (2000) *J Am Chem Soc* 122:5258–5261
- Liu A, Hidajat K, Kawi S, Zhao D (2000) *Chem Commun* 13:1145–1146
- Walcarius A, Mercier L (2010) *J Mater Chem* 20:4478–4511
- Wang W, Grozea D, Kohli S, Perovic DD, Ozin GA (2011) *ACS Nano* 5:1267–1275
- Moorthy MS, Park S-S, Fuping D, Hong S-H, Selvaraj M, Ha C-S (2012) *J Mater Chem* 22:9100–9108
- Karimi B, Khorasani M, Bakhshandeh Rostami F, Elhamifar D, Vali H (2015) *ChemPlusChem* 80:990–999
- Veisi H, Azadbakht R, Saeidifar F, Abdi MR (2017) *Catal Lett* 147:976–986
- Sadeghzadeh SM (2016) *Catal Lett* 146:2555–2565
- Hajjami M, Rahmani S (2015) *J Porous Mater* 22:1265–1274
- Hajjami M, Kolivand S (2016) *Appl Organomet Chem* 30:282–288
- Hajjami M, Shiri L, Jahanbakhshi A (2015) *Appl Organomet Chem* 29:668–673

38. Modak A, Mondal J, Bhaumik A (2012) *Green Chem* 14:2840–2855
39. Modak A, Nandi M, Bhaumik A (2012) *Catal Today* 198:45–51
40. Verma S, Nandi M, Modak A, Jain SL, Bhaumik A (2011) *Adv Synth Catal* 353:1897–1902
41. Horiuchi Y, Do Van D, Yonezawa Y, Saito M, Dohshi S, Kim T-H, Matsuoka M (2015) *RSC Adv* 5:72653–72658
42. Zhu F-X, Wang W, Li H-X (2011) *J Am Chem Soc* 133:11632–11640
43. Huang J, Zhu F, He W, Zhang F, Wang W, Li H (2010) *J Am Chem Soc* 132:1492–1493
44. Yang Q, Liu J, Zhang L, Li C (2009) *J Mater Chem* 19:945–1955
45. Hoffmann F, Fröba M (2011) *Chem Soc Rev* 40:608–620
46. Sasidharan M, Bhaumik A (2013) *ACS Appl Mater Interfaces* 5:2618–2625
47. Elhamifar D, Karimi B, Moradi A, Rastegar J (2014) *ChemPlusChem* 79:1147–1152
48. Wahab MA, Kim I, Ha C-S (2004) *J Solid State Chem* 177:3439–3447
49. Elhamifar D, Nasr-Esfahani M, Karimi B, Moshkelgosha R, Shábani A (2014) *ChemCatChem* 6:2593–2599
50. Na W, Wei Q, Lan J-N, Nie Z-R, Sun H, Li Q-Y (2010) *Microporous Mesoporous Mater* 134:72–78
51. Elhamifar D, Kazempoor S, Karimi B (2016) *Catal Sci Technol* 6:4318–4326
52. Elhamifar D, Kazempoor S (2016) *J Mol Catal A* 415:74–81
53. Shylesh S, Wagener A, Seifert A, Ernst S, Thiel WR (2010) *Angew Chem Int Ed* 49:184–187
54. Wei Q, Liu L, Nie Z-R, Chen H-Q, Wang Y-L, Li Q-Y, Zou J-X (2007) *Microporous Mesoporous Mater* 101:381–387
55. Cho E-B, Kim D, Jaroniec M (2009) *Langmuir* 25:13258–13263
56. Foye W (1991) Padova, Italy 416
57. Wu JY-C, Fong W-F, Zhang J-X, Leung C-H, Kwong H-L, Yang M-S, Li D, Cheung H-Y (2003) *Eur J Pharmacol* 473:9–17
58. Raj T, Bhatia RK, Sharma M, Saxena A, Ishar M (2010) *Eur J Med Chem* 45:790–794
59. Rueping M, Sugiono E, Merino E (2008) *Chemistry A* 14:6329–6332
60. Moon D-O, Kim K-C, Jin C-Y, Han M-H, Park C, Lee K-J, Park Y-M, Choi YH, Kim G-Y (2007) *Int Immunopharmacol* 7:222–229
61. Konkoy C, Fick D, Cai S, Lan N, Keana J, Int PCT (2000) Appl WO 0075123:2001, p. 29313a Chem. Abstr
62. Shaterian H, Oveisi A (2011) *J Iran Chem Soc* 8:545–552
63. Brahmachari G, Banerjee B (2013) *ACS Sustain Chem Eng* 2:411–422
64. Elhamifar D, Elhamifar D, Shojaeipoor F (2017) *J Mol Catal A* 426:198–204
65. Elhamifar D, Ardeshtirfard H (2017) *J Colloid Interface Sci* 505:1177–1184
66. Elhamifar D, Yari O, Karimi B (2017) *J Colloid Interface Sci* 500:212–219
67. Elhamifar D, Badin P, Karimipoor G (2017) *J Colloid Interface Sci* 499:120–127
68. Elhamifar D, Ramazani Z, Norouzi M, Mirbagheri R (2018) *J Colloid Interface Sci* 511:392–401
69. Norouzi M, Elhamifar D, Mirbagheri R, Ramazani Z (2018) *J Taiwan Inst Chem Eng* 89:234–244
70. Elhamifar D, Shabani A (2014) *Chem Eur J* 20:3212–3217
71. Dekamin MG, Alikhani M, Javanshir S (2016) *Green Chem Lett Rev* 9:96–105
72. Dekamin MG, Peyman SZ, Karimi Z, Javanshir S, Naimi-Jamal MR, Barikani M (2016) *Int J Biol Macromol* 87:172–179
73. Khurana JM, Nand B, Saluja P (2010) *Tetrahedron* 66:5637–5641
74. Khan AT, Lal M, Ali S, Khan MM (2011) *Tetrahedron Lett* 52:5327–5332
75. Pore D, Undale K, Dongare B, Desai U (2009) *Catal Lett* 132:104–108
76. Abdolmohammadi S, Balalaie S (2007) *Tetrahedron Lett* 48:3299–3303
77. Dekamin MG, Eslami M, Maleki A (2013) *Tetrahedron* 69:1074–1085
78. Abdollahi-Alibeik M, Nezampour F (2013) *React Kinet Mech Catal* 108:213–229
79. Moghaddas M, Davoodnia A (2015) *Res Chem Intermed* 41:4373–4386
80. Esmailpour M, Javidi J, Dehghani F, Dodeji FN (2015) *RSC Adv* 33(5):26625
81. Niknam K, Jamali A (2012) *Chin J Catal* 33:1840–49
82. Sedaghat M, Booshehri MR, Nazarifar M, Farhadi F (2014) *Appl Clay Sci* 95:55–59
83. Tabatabaieian K, Heidari H, Mamaghani M, Mahmoodi NO (2012) *Appl Organomet Chem* 26:56–61
84. Tayebee R, Pejhan A, Ramshini H, Maleki B, Erfaninia N, Tabatabaie Z, Esmaeili E (2018) *Appl Organomet Chem* 32:e3924
85. Khoobi M, Ma'mani L, Rezazadeh F, Zareie Z, Foroumadi A, Ramazani A, Shafiee A (2012) *J Mol Catal A* 359:74–80
86. Hojati SF, Amiri A, MoeiniEghbali N, Mohamadi S (2018) *Appl Organomet Chem* 32(4):e4235

**Publisher's Note** Springer Nature remains neutral with regard to jurisdictional claims in published maps and institutional affiliations.

## Affiliations

Meysam Norouzi<sup>1</sup> · Dawood Elhamifar<sup>1</sup>

✉ Dawood Elhamifar  
d.elhamifar@yu.ac.ir

<sup>1</sup> Department of Chemistry, Yasouj University,  
75918-74831 Yasouj, Iran